Charge state of vacancy defects in Eu-doped GaN

B. Mitchell,[1,2,*] N. Hernandez,[3] D. Lee,[4] A. Koizumi,[2] Y. Fujiwara,[2] and V. Dierolf[3]
[1]*Department of Physics, West Chester University, West Chester, Pennsylvania 19383, USA*
[2]*Division of Materials and Manufacturing Science, Graduate School of Engineering, Osaka University, 2-1 Yamadaoka, Suita, Osaka 565-0871, Japan*
[3]*Department of Physics, Lehigh University, Bethlehem, Pennsylvania 18015, USA*
[4]*Department of Materials Science and Engineering, Pohang University of Science and Technology (POSTECH), Pohang, Gyeongbuk 37673, South Korea*
(Received 15 April 2017; revised manuscript received 10 August 2017; published 31 August 2017)

Eu ions have been doped into GaN in order to achieve red luminescence under current injection, where coupling between the Eu ions and intrinsic defects such as vacancies are known to play an important role. However, the charge state of the vacancies and the impact it would have on the optical and magnetic properties of the Eu ions have not been explored. Through a combination of first-principle calculations and experimental results, the influence of the charge state of the defect environment surrounding the Eu ions has been investigated. We have identified two Eu centers that are related through the charge state of a local vacancy defect. These two centers were found to exhibit a mutual metastability, such that each center can be excited in one configuration and emit as the other. This metastability was found to be dependent on temperature and the wavelength of the excitation laser. Furthermore, one of these centers was found to have an effective magnetic g factor that is substantially larger than what is expected for an isolated Eu^{3+} ion and is explained by a change in the charge state of the defect environment around the Eu. This prediction could also offer a new explanation for the saturation magnetization previously observed in GaN : Eu and other GaN:RE systems.

DOI: 10.1103/PhysRevB.96.064308

I. INTRODUCTION

Epitaxial layers of GaN doped with europium (Eu) have demonstrated great promise for red light-emitting diodes (LEDs), which would enable the fabrication of an active three-color light source that is solely based on the hexagonal nitride platform [1–8]. The magnetic properties of GaN : Eu and other rare earth (RE)-doped GaN dilute magnetic semiconductor (DMS) systems have also been extensively investigated for spintronic applications [9–15]. It is known that the Eu ions will incorporate into GaN in several defect environments and that these defect environments play an important role on the spectral position of the Eu emission [16–24] and in the ability for the Eu ions to capture energy from the GaN host during the recombination of electrons and holes [7,18,22]. Extensive spectroscopic work has provided ample evidence that the two main emitting centers, referred to as Eu1 and Eu2, are complexes consisting of a Eu ion on a gallium site with either a nitrogen (V_N) or gallium (V_{Ga}) vacancy in close proximity [20,22]. Eu1 has been associated with a V_N, while Eu2, which contributes the most to the emission intensity under current injection, has been associated with a V_{Ga}. These results are in agreement with several theoretical investigations of RE-doped GaN, which have also predicted that RE-V_N and RE-V_{Ga} complexes are stable in GaN and could assist with the enhancement of luminescence due to energy transfer from the GaN host [25–29].

Despite this electrical signature, the charge state of the vacancy, the ability for it to change with temperature, and the impact that this would have on the optical properties of the Eu ions have not been addressed experimentally. Since the properties of the Eu ions are sensitive to local perturbations, it is possible that charge capture by a defect could strongly influence the optical and magnetic properties. Thus, it would be advantageous to consider the dynamics of the charge states of intrinsic defects in GaN, namely V_N and V_{Ga}, whose properties have been extensively investigated [30,31]. Van de Walle and Neugebauer have shown that these vacancies can exist in several charge states as a function of the Fermi level, which is correlated with temperature [30]. Nitrogen vacancies can exist in one of two charge states (0 or +1), while gallium vacancies behave as triple acceptors and can exist in one of four charge states (−3, −2, −1, and 0). The different charge states for the V_{Ga} are located within a narrow range of Fermi levels in the lowest third of the band gap and could coexist at certain temperatures and under certain excitation conditions. Furthermore, V_{Ga} has a magnetic moment in the neutral state, which diminishes at room temperature once the vacancy captures negative carriers [31,32]. This magnetic moment could influence the Eu ions if they locally coupled as a defect complex. An extensive theoretical investigation of RE defect pairs in GaN was performed by Sanna *et al.* using local-density approximation (LDA) with a Hubbard U correction or LDA + U [28]. Sanna *et al.* reported on the formation energies of the RE-vacancy complexes in different charge states and noted that, in the case of Eu_{Ga}-V_{Ga} complexes, the charge transitions of the vacancies take place at very similar Fermi energies as compared to isolated V_{Ga}, independent of the RE. These complexes were all found to be quite stable. However, the atomic displacements of the RE ions and the spatial distribution of the electron charge density as a function of charge state were not discussed.

In a previous study, an anomalous behavior was found in the luminescence from a Eu center labeled OMVPE8 [33]. While the intensity of the other Eu centers was quenched

*bmitchell@wcupa.edu

with increasing temperature, the emission from OMVPE8 was found to increase, reaching a maximum intensity at around 140 K. However, no explanation for this observation was given. Time-resolved photoluminescence results showed an "afterglow" effect, where the emission from OMVPE8 increased after the laser pulse had ended. This was explained by introducing an arbitrary excitation channel, which was "blocked" during laser excitation, but could excite OMVPE8 once the laser excitation had ceased. An alternative explanation was also offered where OMVPE8 captured a charge, which inhibited energy transfer during laser excitation. However, the latter explanation was argued away. In addition, two other studies on the properties of the luminescence from GaN : Eu under the application of a magnetic field showed that OMVPE8 exhibited a curiously large effective g factor of $\sim$6, which was estimated by analyzing the Zeeman splitting of the emission peaks [34,35]. This is much larger than the effective g factor measured for the other Eu centers, which ranged from $\sim$1.9–2.6. Neither of the studies offered an explanation as to the mechanism behind the large effective g factor.

In this paper, we explore the question of how the charge state of the Eu_{Ga}-V_{Ga} complex influences the optical and magnetic properties of the Eu^{3+} ions. For this, density functional theory $+U$ (DFT $+ U$) was employed, and it is shown that a change in the charge state of the gallium vacancy will significantly perturb the Eu ions away from the substitutional Ga site, as well as influence the charge distribution within the defect complex. This prediction was confirmed experimentally utilizing temperature-dependent spectroscopy with various laser excitation sources, as well as current injection. It was concluded that the Eu2 and OMVPE8 centers have the same basic defect configuration, distinct only by charge state of a local V_{Ga}.

II. METHODOLOGY

A. Crystal growth

The samples used in this paper were all grown on sapphire (0001) substrates by OMVPE (Taiyo Nippon Sanso SR-2000). The samples consist of a 10-nm-thick GaN capping layer, a 400-nm-thick GaN : Eu layer, a 2–3-nm-thick undoped GaN layer, and a 30-nm-thick GaN buffer layer grown on the sapphire (0001) substrate at a temperature of 1030 °C. To test the effects of pressure, two samples were grown at reactor pressures of 10 and 100 kPa and had Eu concentrations of $7 \times 10^{19}\,cm^{-3}$ and $3 \times 10^{19}\,cm^{-3}$, as determined by secondary ion mass spectroscopy, respectively. Samples with varied V/III ratios are also explored. These samples were grown at 100 kPa, with N/Ga source flow rate ratios of 3200 and 6400, and Eu concentrations of 6×10^{19} and $4 \times 10^{19}\,cm^{-3}$, respectively. This ratio was controlled by altering the NH_3 flow rate. Additional details on the OMVPE growth of GaN : Eu can be found elsewhere [7,17,22].

B. Multiple laser excitation emission spectroscopy

In order to explore the spectroscopic properties of the samples, several excitation methods were used. This included excitation: (1) of the GaN host using above-band gap light, (2) of deep traps using below-band gap (BBG) light, (3) of the distinct Eu ion defect configurations using light that is resonant with the $^5F_0$ to $^5D_0$ transition within the $4f$ manifold, and (4) of combinations of the above cases. A tunable dye laser, using Rhodamine 6G, was used for resonant excitation, a 325 nm He-Cd laser was used for above-band gap excitation [ultraviolet (UV)], and a (1W) 532 nm laser was used for excitation into BBG defect levels. These lasers were used individually, as well as simultaneously utilizing a homemade fiber-based, dual-excitation confocal microscope. To control the temperature, samples were mounted inside a closed cycle cryostat. All spectra were collected using a 0.5 m monochromator equipped with a charge coupled device (CCD) camera. To explore the relative ratios and dynamics of the Eu incorporation centers, the technique of combined excitation emission spectroscopy (CEES) was employed, in which the various centers are excited selectively by tuning the laser to their respective resonance. Details about this technique and more results applying it to GaN : Eu can be found elsewhere [18,22].

C. Pulse-driven emission spectroscopy

The optical properties of the samples under current injection and the nature of the charge capture potentials for each incorporation center were investigated using a technique called pulse-driven emission spectroscopy (PDES) [36–38]. In this technique, a rectangular wave (duty cycle 0.5) from a signal generator (GW Instek, Co., Ltd., AFG-2005) was used to pulse-drive a GaN : Eu LED with a fixed pulse voltage of 6.0 V. The emission from the LED was detected using a spectrometer (Princeton Instruments, Acton SP2500) with a CCD (Princeton Instruments, PIXIS 100), with a fixed integration time of 20 s. The samples were cooled using a closed-cycle cryostat with vacuum feedthroughs for the electrical connections. The GaN : Eu LED structure was fabricated on a sapphire (0001) wafer by OMVPE. The LED consisted of a 300-nm-thick GaN : Eu active layer (Eu concentration $4.5 \times 10^{19}\,cm^{-3}$), which was inserted between a p-type Mg-doped GaN layer (hole concentration $5.6 \times 10^{17}\,cm^{-3}$) and an n-type Si-doped GaN layer (electron concentration $3 \times 10^{18}\,cm^{-3}$). See Refs. [36–38] and Ref. [3] for more information on PDES and the structure of the LED, respectively.

D. Theoretical calculations

Density functional theory $+U$ calculations are used to investigate changes in the atomic displacement of the Eu^{3+} ion in the Eu_{Ga}-V_{Ga} complex (Eu2 center) under different charge states, as well as the spatial distribution of the charge density around the Eu-V_{Ga} complex. We perform the DFT $+ U$ calculations with the generalized gradient approximation (GGA) of the Perdew-Burke-Ernzerhof (PBE) for the exchange and correlation energy [39]. A plane-wave basis set with the projector augmented wave (PAW) method implemented in the Vienna *ab initio* Simulation Package (VASP) code is used to represent the interaction between electron and ion core [40]. An energy cutoff of up to 500 eV is used for the plane-wave representation of the wave functions. Atomic structures are relaxed until all Hellman-Feynman forces are below 0.01 eV/Å. Monkhorst-Pack k-point sampling with a grid of $2 \times 2 \times 2$ was used for the Brillouin zone integration [41].

The bulk GaN system is constructed by an 128-atom supercell ($4 \times 4 \times 2$ unit-cell), and the Eu ion is assumed to replace the Ga site with a neutral charge state. A Hubbard U correction term ($U = 6.8$ eV) is applied to the Eu ion in order to properly reproduce the strong onsite Columbic repulsion of highly localized $4f$ electrons [28]. The pseudopotential approach was used [29], where the configurations $3d^{10}\,4s^2 4p^1$, $2s^2 2p^3$, and $5s^2 5p^6 4f^7 6s^2$ were treated as valence electrons for Ga, N, and Eu, respectively. The neutralizing background charge of the opposite sign is implicitly introduced to compensate for the charged system.

III. RESULTS

A. DFT + U calculations of V_{Ga}-Eu complexes with different charge states

Since the Eu2 center has been associated with a V_{Ga} as a second nearest neighbor, the behavior of V_{Ga} and Eu-V_{Ga} complexes in different charge states should be explored. As mentioned previously, the charge state of isolated V_{Ga} and Eu-V_{Ga} complexes have been shown to change from 0 to 3^- as a function of Fermi level, which increases with temperature [28,30]. In the case of the Eu-V_{Ga} complex, the Eu is assumed to remain in the trivalent oxidation state, with the V_{Ga} capturing the charges. This means that the V_{Ga} captures free electrons, which would change the distribution of the charge density around the vacancy. Figures 1(a)–1(c) show the spatial distribution of the electron charge density around a V_{Ga} for the case where the vacancy has captured one to three excess electrons, respectively. The charge density is delocalized around the vacancy in a similar and somewhat symmetric way for each of the three cases. Overall, the shape of the charge distribution does not change appreciably, only the total magnitude of the charge.

This situation changes significantly, when Eu-V_{Ga} defect complexes are considered. Figures 1(e)–1(f) show the spatial distribution of the electron charge density for such complexes. For these calculations, it was assumed that the V_{Ga} had captured electrons from the GaN host. Focusing first on the position of the Eu ion within the lattice, Figs. 1(e)–1(f) show that the perturbation by the vacancy displaces the Eu atom from the gallium site, where it should be located in the absence of a perturbation. The degree of this displacement depends on the charge state of the complex. A similar observation was made on Mg-H-Eu complexes in GaN : Eu that was codoped with Mg [20,21]. In these samples, a new Mg-H-related center was observed that had a significantly blue shifted emission spectra, relative to the standard Eu emission peaks. Thus, the appearance of emission peaks that differ from each other should be expected as a signature of defect complexes of different charge states.

As for the distribution of the charge, we note that the charge density is no longer symmetric with the presence of the Eu, and the spatial distribution changes shape as more electrons are added. These complexes do exhibit a magnetic moment that varies in strength depending on the number of excess electrons that have been captured and have orientations that are different than those calculated for a V_{Ga} alone. Similar calculations were performed on V_N and Eu-V_N complexes, since they are also present in GaN : Eu [22]. No magnetic moment was found for the V_N or the Eu-V_N for any charge state. Thus, the observed magnetic moment is unique to the V_{Ga} and Eu-V_{Ga} defect complexes. The question remains: how are the optical and magnetic properties of the Eu ion influenced by the atomic displacement of the Eu ion and the change in the electron distribution around the V_{Ga} to which it is coupled?

B. Temperature-dependent resonant excitation

To answer this question and explore the predictions in GaN:Eu, CEES measurements were performed at several temperatures. The site selectivity of the CEES technique

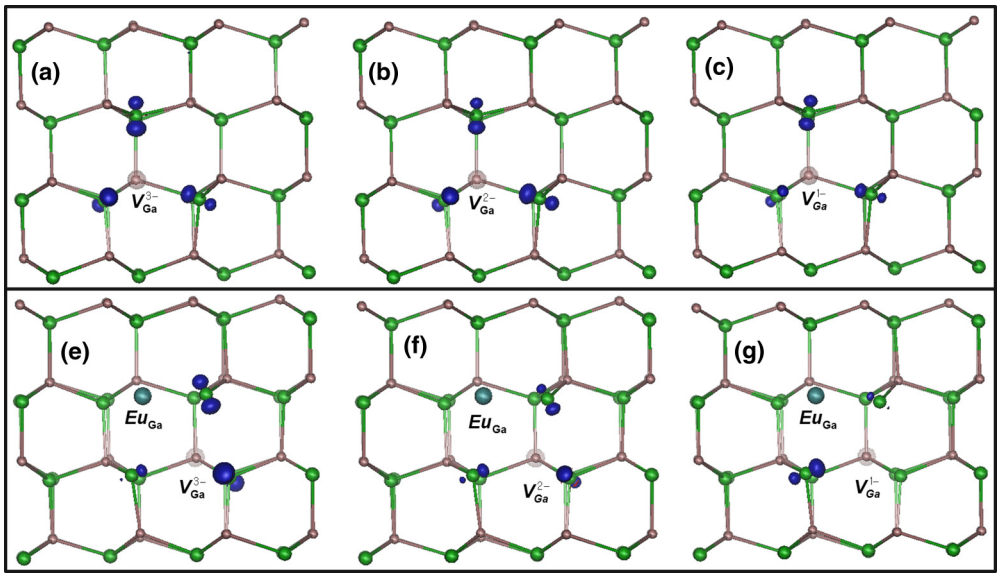

FIG. 1. (a)–(c) Spatial distribution of the electron charge density around a V_{Ga} for the case where the vacancy has captured one to three excess electrons, respectively. (e)–(g) Spatial distribution of the electron charge density around V_{Ga}-Eu complexes which have captured one to three excess electrons, respectively. The isosurfaces of charge density are plotted at 0.1 e/Å^3 for V_{Ga}^{2-} and V_{Ga}^{3-} and at 0.06 e/Å^3 for V_{Ga}^{1-}.

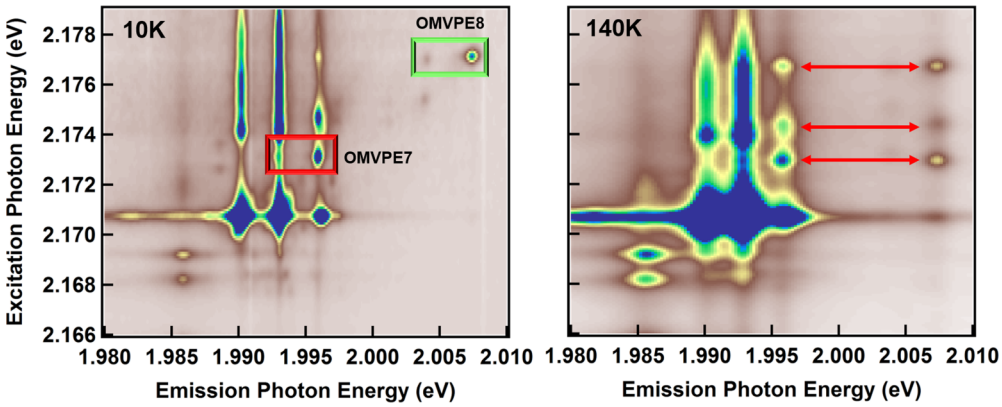

FIG. 2. CEES maps of a GaN : Eu sample grown with a V/III ratio of 6400 at 10 and 140 K. At 140 K, the emission from Eu2 occurs as the resonant excitation energy of OMVPE8 and vice versa, suggesting a link between the two centers.

enables the distinction between individual Eu centers, which have different local perturbations. Figure 2 shows the CEES results for a GaN:Eu sample with a V/III ratio of 6400, at 10 and 140 K. These samples are known to have a larger relative concentration of Eu2 [22]. At 10 K, Eu2 shows two emission peaks, with the brightest one at 1.996 eV. In addition to the resonant excitation energy of Eu2 (∼2.173 eV), there is also a phonon replica at ∼2.175 eV. Another center labeled OMVPE8 is also shown, which has an excitation energy of ∼2.177 eV, and also contains two emission peaks. The brighter emission peak from OMVPE8 is at 2.007 eV. It should be noted that the two peaks associated with OMVPE8 are separated by a similar energy difference as the two peaks associated with Eu2.

At 140 K, emission at 2.008 eV can be seen for excitation energies formerly associated with Eu2 (2.173 and 2.175 eV). Similarly, emission at 1.996 eV can be observed under an excitation energy of 2.177 eV, which was formerly associated with OMVPE8. Thus, it appears that exciting Eu2 can lead to emission from OMVPE8 and vice versa.

To shed more light on this observation, similar measurements were performed on a GaN:Eu sample with a V/III ratio of 3200. The CEES map of this sample contains a distinct defect-related excitation feature, which extends through a range above and below the resonant excitation energies of the Eu^{3+} ions. This "stripe" has been associated with an extended defect center. After its excitation, energy can be transferred to Eu centers, preferentially to those that capture energy from the GaN host most effectively [18,22]. At 10 K, this is the Eu2 center complex in most samples. Thus, the presence of such defects is reflected in low-temperature CEES maps [Fig. 3 (left)] as an excitation stripe that appears at the Eu2 emission energy. A weak emission from OMVPE8 can also be observed at 10 K, with a very weak stripe that can barely be detected above noise. However, once the sample temperature was raised to 140 K, the stripe can be seen at the spectral positions associated with both Eu2 and OMVPE8. Furthermore, an emission peak at 2.007 eV can be seen at the excitation energy of Eu2, in agreement with the observations in Fig. 2. Independent of the excitation mode, both the Eu2 and the OMVPE8 center are excited simultaneously at temperatures above 140 K.

These observations can readily by explained if we assume that the Eu2 and OMVPE8 centers have the same defect configuration and are distinct only in the charge state of the complex, as was predicted by the DFT + U calculations in Sec. III A. The capturing of a charge perturbs the Eu ion and gives rise to blue shifted excitation and emission energies. When the sample temperature is increased, more charges become available from other charge traps, increasing the likelihood of the V_{Ga}-Eu complex to have captured charges.

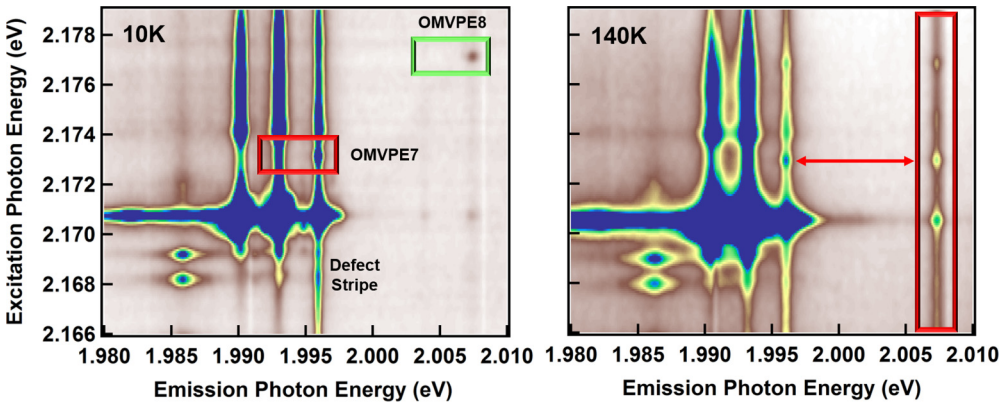

FIG. 3. CEES maps of a GaN : Eu sample grown with a V/III ratio of 3200 at 10 and 140 K. At 140 K, the emission from the defect stripe is shared between Eu2 and OMVPE8. Also, the emission from Eu2 occurs as the resonant excitation energy of OMVPE8 and vice versa, as it did in Fig. 1.

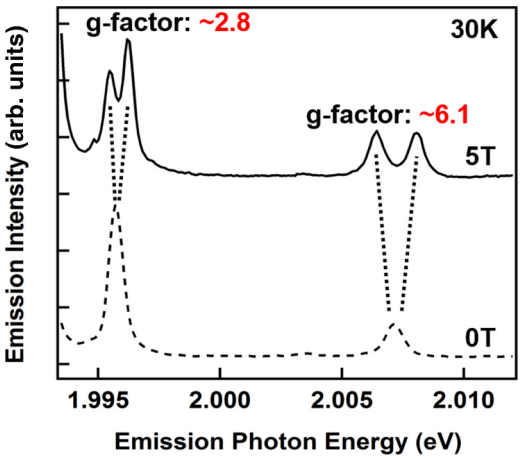

FIG. 4. Emission profiles taken at the resonant excitation energy of OMVPE8 under the application of magnetic field of 0 and 5 T. The effective g factors determined from these emission lines were calculated to be 2.8 and 6.1 for Eu2 and OMVPE8, respectively. Both of these values are significantly greater than the pure g factor value of 1.5 expected for the transition between $^5D_0$ and $^7F_2$ obtained from the Landé formula in the LS coupling scheme.

However, at this temperature, it also becomes more likely that the charge is released from the complex either thermally and under optical excitation of the complex. As a result, the complex could be excited as Eu2/OMVPE8 and then capture/release an electron, and emit as the other center. In the spirit of the new assignment, OMVPE8 will be hereafter referred to as Eu2*, which indicates that Eu2* is the Eu2 center with an excess electron. It is assumed that Eu2* is the charged center because Eu-V_{Ga} with excess electrons are predicted to occur more readily at elevated temperatures [28].

Next, the emission from Eu2 and Eu2* are explored under application of a magnetic field in order to investigate the magnetic properties of the centers. While similar experiments have been performed on GaN:Eu, it is necessary to confirm these results on the samples used in this paper [34,35]. Since the sample with a V/III ratio of 6400 shows more Eu2 and Eu2* emission, it should be easier to compare the effective g factors obtained from the Zeeman splitting of their brightest emission lines. This observation results from the splitting of the $^7F_2$ multiplet, since the $^5D_0$ should not split due to the magnetic field. Figure 4 shows the emission spectra from Eu2 and Eu2* under application of a 0 and 5 T magnetic field. It can easily be seen that the Zeeman splitting of Eu2 is much less than that from Eu2*. For the $^7F_2$ multiplet, both S and L have quantum numbers of 3. In the LS coupling scheme, using the Landé formula, the g factor of the $^7F_2$ multiplet should be exactly 1.5. Interaction with the crystal field will cause the measured g factor to deviate from this value, as can be seen from the previously reported effective g factors of Eu1 (∼1.8–2) [34,35]. The effective g factors obtained from the emission spectra in Fig. 4 are 2.8 and 6.1 for Eu2 and Eu2*, respectively. While these values are within reasonable agreement with those previously reported [34,35], it remains that these effective g factors, especially from Eu2*, are comparatively high. The unusually large effective g factor measured for the 2.007 eV emission line of Eu2* (∼6.1) indicates that this transition is related to a state with a higher spin than would be expected for an isolated Eu^{3+} center. Considering the magnetic moment of the Eu-V_{Ga} complexes obtained from DFT + U, it is possible that the higher spin could be attributed to a spin coupling between the Eu-V_{Ga} defect complex as a whole, and the spin of the electronic states of the Eu^{3+} ion.

C. Temperature-dependent pulse-driven electroluminescence spectroscopy

In a previous section, it was proposed that once excited, Eu2 or Eu2* could capture/release a carrier and emit either as one or the other. While the excitation of Eu2 can be distinguished from the excitation of Eu2* under resonant excitation, this is not the case for excitation as a result of energy transfer from the recombination of electrons and holes. This occurs when the GaN host is excited above the band gap or during current injection. In this case, the excitation of Eu2 should not be distinguishable from Eu2* at temperatures ∼140 K or above. Pulse-driven emission spectroscopy is a measurement that has been used to distinguish the carrier capture potential for the different centers in GaN : Eu by detecting their emission intensity as a function of the alternating supply voltage frequency [36,37]. It was found that each center exhibits a unique frequency response [38]. Figure 5(a) shows the integrate emission intensity from Eu2 and Eu2* as a function of the supply voltage frequency at 110 K. The shape of the frequency response curves of Eu2 and Eu2* are quite different, as expected.

Once the temperature is increased to 140 K, the frequency response curves become more similar in shape [Fig. 5(b)]. At 180 K, the frequency response curves practically overlap, which indicates that the excitation of Eu2 has become indistinguishable from Eu2*. This is because PDES simply measures the integrated emission intensity from each center. Since the excitation of Eu2 could lead to either Eu2 or Eu2* emission, this would make it impossible to discern whether the emission from Eu2 came from the excitation of Eu2 or Eu2*. This also means that the emission intensity of the two centers should become comparable at elevated temperatures. Figure 5(d) shows the emission spectra for the peak frequency of Eu2* at 110 and 180 K. The ratio of the emission intensity from Eu2 and Eu2* becomes lower as the temperature increases, and it appears as though the emission from each center is reaching an equilibrium. It seems reasonable that, as the temperature increases, more intrinsic free carriers are mobile in the GaN host, and the carrier capture/release that leads to the transformations between Eu2 and Eu2* occurs more frequently.

D. Multiple excitation emission spectroscopy

Up until now, the transformation of Eu2 into Eu2* or vice versa has been inferred from observation of emission peaks observed in CEES or the overlap of the frequency response curves from PDES. In both of these experiments, this behavior was only observed for elevated temperatures, where formation of Eu2* becomes more preferable. It is also expected that the formation of Eu2* should increase if charge carriers are made more available. To study such the dynamic change from Eu2 to Eu2*, a dual excitation experiment was performed at

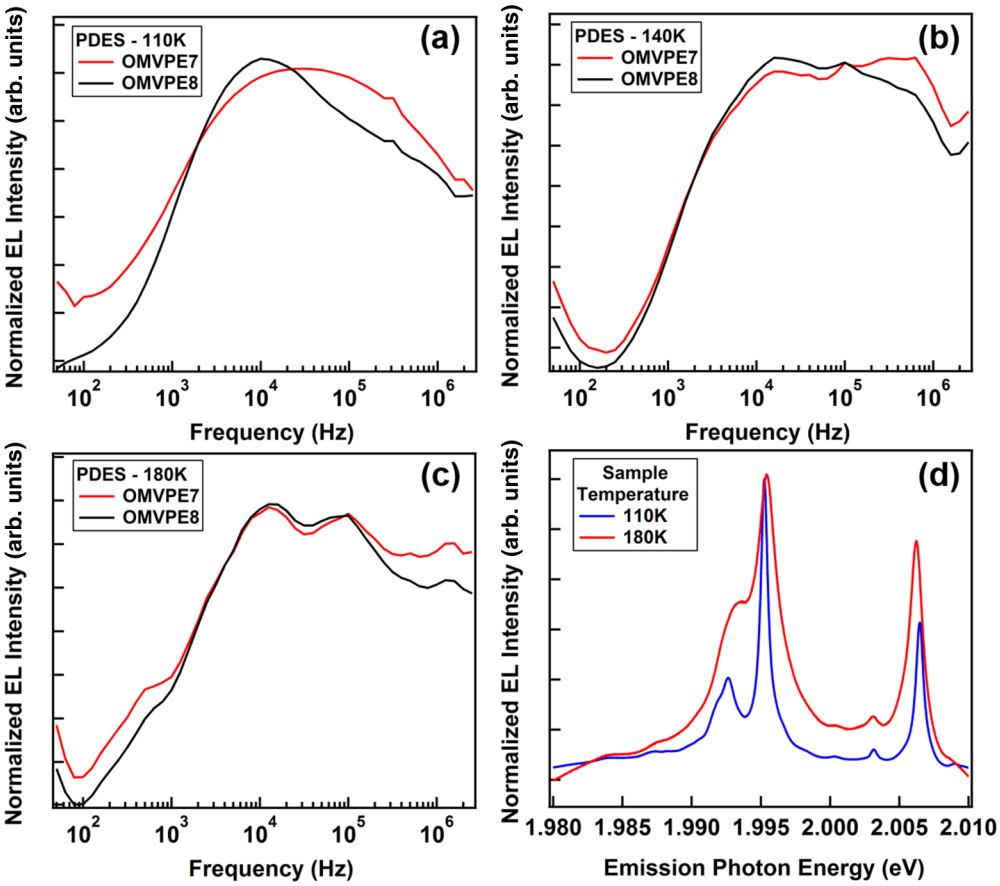

FIG. 5. Frequency response curves for Eu2 and Eu2* acquired from PDES measurements taken at: (a) 110 K, (b) 140 K, and (c) 180 K. The emission spectra at the peak frequency of Eu2* at 110 and 180 K is given in (d).

10 K. At this low temperature, Eu2 dominates the emission spectra under 325 nm (UV) excitation. To access additional charges, the defect complex (stripe defect) discussed above is utilized. Under excitation, a charge is released. This center is most pronounced in the sample with a V/III ratio of 3200. A BBG 532 nm laser was used to excite this center. The UV and BBG excitation beams were overlapped using a confocal microscope, and the emission was collected under UV excitation alone, as well as the combined excitation of UV and BBG. The power of the BBG laser was increased from 10 to 50 mW, and the results are shown in Fig. 6.

The two emission profiles nearly overlap for a BBG excitation power of 10 mW. However, for BBG excitation powers of 30 and 50 mW, the emission from Eu2 goes down, and the emission from Eu2* goes up. This demonstrates that the Eu2/Eu2* ratio can be changed by supplying charges,

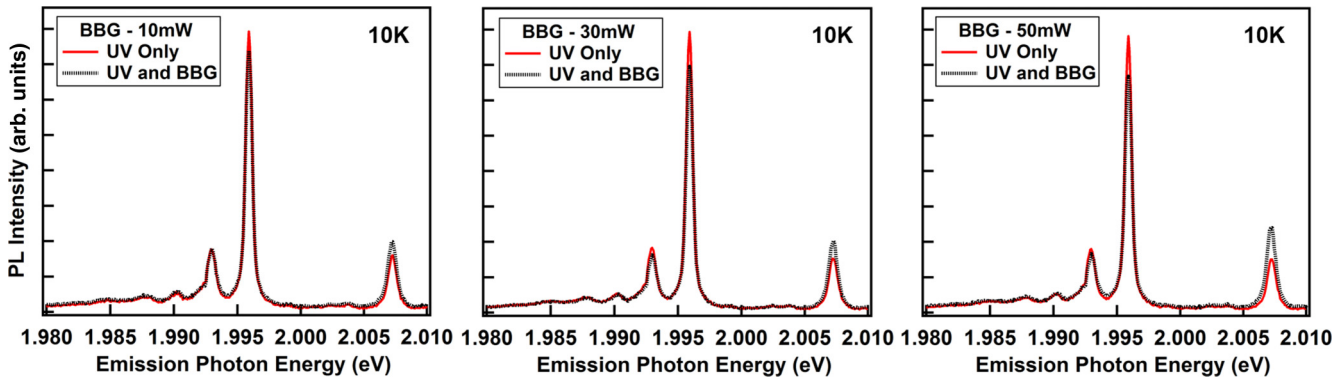

FIG. 6. Comparison of the emission spectra of the GaN : Eu sample with a V/III ratio of 3200 under 325 nm (UV) excitation alone and overlapped with 532 nm (BBG) excitation. The 532 nm laser can excite the Eu^{3+} ions through the defect stripe observed in Fig. 3. The excitation power of the 532 nm laser was increased from 10 to 50 mW at 10 K. The conversion of Eu2 into Eu2* is clearly observed for a BBG excitation power of 50 mW.

which confirms our assumption that these two centers are only distinct in their charge state.

IV. DISCUSSION

The assumption that Eu2 and OMVPE8 are the same center linked through the charge state of a localized V_{Ga} can easily explain the presented results. However, these results can also be used explain the afterglow behavior observed by Wakamatsu *et al.*, which they attributed to an arbitrarily defined defect trap level that could transfer energy to OMVPE8 [33]. The fact that emission can be seen from one center under excitation of the other at 140 K suggests that the capture and release of charges occurs on time scales much shorter than the relatively long lifetime of the $^5D_0$ state of the Eu^{3+} ions ($\sim$250 μs). Moreover, under excitation with energetic electrons, the Eu2/Eu2* ratio leans toward Eu2. However, after the UV light is switched off, thermal equilibrium is quickly reestablished for $T > 140$ K, giving rise to observed increase of Eu2* emission.

While at elevated temperatures the Eu2 and Eu2* centers have almost the same probability to exist, it is found that Eu2 is much more favorable at low temperature due to the lack of free carriers. Such carriers are trapped at other defects at these temperatures, and both Eu2 and Eu2* are stable. However, freeing up charges, either by raising the temperature or exciting the sample above the bandgap, facilitates the conversion of Eu2 into Eu2*.

Furthermore, our DFT + U calculations predicted that a Eu-V_{Ga} complex should have an anomalous magnetic moment and that the moment changes with the capture of electrons. This prediction could explain the abnormally high effective g factors for Eu2, and especially Eu2*. The effective g factor is measured for the $^7F_2$ state, and due to the fact that ground state has no magnetic moment, the high effective g factors could only result from a coupling to an external magnetic moment. The number of these centers depends on the growth conditions of the GaN : Eu. These results could also offer an explanation for the magnetic behavior observed in other GaN : RE systems. For example, large magnetizations were reported in GaN : Gd [10,42]. In addition, room-temperature saturation magnetization was measured in GaN : Er epilayers, where the strength of the magnetization was correlated with the growth substrate, and could be increased with laser excitation [13,15].

Several models have been proposed to explain the ferromagnetic behavior in other GaN : RE DMS systems. Defects such as gallium vacancies and vacancy clusters were proposed as possible sources for this large magnetization [32,43,44]. For the case of clusters, the role of Gd was to perturb the lattice and facilitate the formation of vacancy clusters. The vacancy clusters remained in the neutral charge state, where the magnetic moment per vacancy was the highest. Other models include the formation of bound magnetic polarons and free carrier mediated Ruderman-Kittel-Kasuya-Yoshida (RKKY)-type interactions [10,45,46]. These explanations require a coupling between the spins of free carriers and magnetic dopants; however, room-temperature saturation magnetization was also measured in GaN : Eu, which was reported to be strongly dependent on the growth parameters. Since the ground state of Eu^{3+} has no magnetic moment, this magnetism was unexpected and explained by the presence of Eu^{2+}, although no direct evidence for this explanation was offered. In light of the results revealed in this paper, it is possible that the formation of charged vacancy-related defect complexes such as Eu2* could be responsible for the previously measured saturation magnetization in GaN : Eu. Such a phenomena may also enhance the magnetic moments in other GaN : RE systems such as GaN : Er. The magnetization in both GaN : Er and GaN : Eu was observed to increase with laser excitation [13,14]. In our samples, laser excitation drives the formation of Eu2$*$ centers, which have a larger effective g factor. This was attributed to the coupling of a Eu ion with an external magnetic moment, which resulted from the formation of the charged defect complex. Thus, laser excitation could induce the formation of centers with magnetic moments of sufficient strength to increase the overall magnetization of the material.

V. CONCLUSIONS

A connection between two centers previously labeled Eu2 and OMVPE8, distinguishable only by the charge state of a local V_{Ga} defect, was revealed. Density functional theory $+U$ calculations predict that the Eu-V_{Ga} complex could capture free charges and that this would significantly perturb the Eu atom away from its neutral lattice position, leading to a blue shift in emission. Using resonant excitation, it was shown that one of these centers could be excited resonantly, yet emit as the other center. Pulse-driven emission spectroscopy and dual excitation experiments revealed that these two centers can actually be converted into each other and that the excitation of each center becomes indistinguishable at elevated temperatures. It was suggested that this was a result of free carriers being captured/released several times within the emission lifetime of the Eu ions. Furthermore, this complex would have a magnetic moment that varies with the number of captured carriers. In addition to explaining the abnormally large effective g factor observed for Eu2*, this magnetic moment could also explain the magnetization previously measured in GaN : Eu and other GaN : RE systems. Overall, these results reveal useful insights into the relationship between optically active dopants and the charge state of the intrinsic defects to which they are coupled in GaN. Similar behaviors may also be found/exploited in other semiconductor systems.

ACKNOWLEDGMENTS

The authors would like to thank Dr. Masashi Ishii from the National Institute for Materials Science for helpful discussions. The work at Lehigh University was supported by the National Science Foundation Grant (No. ECCS-1140038). The work at Osaka University was partly supported by a Grant-in-Aid for Scientific Research (S) (No. JP24226009) and a Grant-in-Aid for Scientific Research (A) (No. 17H01264) from Japan Society for the Promotion of Science, and by the Photonics Center at Osaka University.

[1] A. J. Steckl, J. C. Heikenfeld, D. S. Lee, M. J. Garter, C. C. Baker, Y. Q. Wang, and R. Jones, IEEE J. Sel. Top. Quantum Electron. **8**, 749 (2002).

[2] L. Bodiou, A. Braud, J.-L. Doualan, R. Moncorgé, J. H. Park, C. Munasinghe, A. J. Steckl, K. Lorenz, E. Alves, and B. Daudin, J. Appl. Phys. **105**, 043104 (2009).

[3] A. Nishikawa, T. Kawasaki, N. Furukawa, Y. Terai, and Y. Fujiwara, Appl. Phys. Express **2**, 071004 (2009).

[4] A. Nishikawa, N. Furukawa, T. Kawasaki, Y. Terai, and Y. Fujiwara, Appl. Phys. Lett. **97**, 051113 (2010).

[5] A. Nishikawa, N. Furukawa, T. Kawasaki, Y. Terai, and Y. Fujiwara, Opt. Mater. **33**, 1071 (2011).

[6] A. Nishikawa, N. Furukawa, D. Lee, K. Kawabata, T. Matsuno, R. Harada, Y. Terai, and Y. Fujiwara, MRS Proc. **1342**, mrss11-1342-v02-08 (2011).

[7] Y. Fujiwara and V. Dierolf, Jpn. J. Appl. Phys. **53**, 05FA13 (2014).

[8] W. Zhu, B. Mitchell, D. Timmerman, A. Uedono, A. Koizumi, and Y. Fujiwara, APL Mater. **4**, 056103 (2016).

[9] M. Hashimoto, A. Yanase, R. Asano, H. Tanaka, and H. Bang, Jpn. J. Appl. Phys. **42**, L1112 (2003).

[10] S. Dhar, O. Brandt, M. Ramsteiner, V. F. Sapega, and K. H. Ploog, Phys. Rev. Lett. **94**, 037205 (2005).

[11] J. Hite, G. T. Thaler, R. Khanna, C. R. Abernathy, S. J. Pearton, J. H. Park, A. J. Steckl, and J. M. Zavada, Appl. Phys. Lett. **89**, 132119 (2006).

[12] J. K. Hite, R. M. Frazier, R. P. Davies, G. T. Thaler, C. R. Abernathy, S. J. Pearton, J. M. Zavada, E. Brown, and U. Hömmerich, J. Electron. Mater. **36**, 391 (2007).

[13] N. Nepal, J. M. Zavada, R. Dahal, C. Ugolini, A. Sedhain, J. Y. Lin, and H. X. Jiang, Appl. Phys. Lett. **95**, 022510 (2009).

[14] R. Wang, A. J. Steckl, N. Nepal, and J. M. Zavada, J. Appl. Phys. **107**, 013901 (2010).

[15] N. T. Woodward, N. Nepal, B. Mitchell, I. W. Feng, J. Li, H. X. Jiang, J. Y. Lin, J. M. Zavada, and V. Dierolf, Appl. Phys. Lett. **99**, 122506 (2011).

[16] V. Kachkanov, M. J. Wallace, G. van der Laan, S. S. Dhesi, S. A. Cavill, Y. Fujiwara, and K. P. O'Donnell, Sci. Rep. **2**, 969 (2012).

[17] R. Wakamatsu, D. Lee, A. Koizumi, V. Dierolf, and Y. Fujiwara, J. Appl. Phys. **114**, 043501 (2013).

[18] N. Woodward, A. Nishikawa, Y. Fujiwara, and V. Dierolf, Opt. Mater. **33**, 1050 (2011).

[19] N. Woodward, J. Poplawsky, B. Mitchell, A. Nishikawa, Y. Fujiwara, and V. Dierolf, Appl. Phys. Lett. **98**, 011102 (2011).

[20] B. Mitchell, D. Lee, D. Lee, A. Koizumi, J. Poplawsky, Y. Fujiwara, and V. Dierolf, Phys. Rev. B **88**, 121202 (2013).

[21] B. Mitchell, D. Lee, D. Lee, Y. Fujiwara, and V. Dierolf, Appl. Phys. Lett. **103**, 242105 (2013).

[22] B. Mitchell, J. Poplawsky, D. Lee, A. Koizumi, Y. Fujiwara, and V. Dierolf, J. Appl. Phys. **115**, 204501 (2014).

[23] W. D. A. M. de Boer, C. McGonigle, T. Gregorkiewicz, Y. Fujiwara, S. Tanabe, and P. Stallinga, Sci. Rep. **4**, 5235 (2014).

[24] H. Peng, C. Lee, H. O. Everitt, C. Munasinghe, D. S. Lee, and A. J. Steckl, J. Appl. Phys. **102**, 073520 (2007).

[25] J.-S. Filhol, R. Jones, M. J. Shaw, and P. R. Briddon, Appl. Phys. Lett. **84**, 2841 (2004).

[26] B. Hourahine, S. Sanna, B. Aradi, C. Köhler, and T. Frauenheim, Physica B **376–377**, 512 (2006).

[27] S. Sanna, B. Hourahine, Th. Frauenheim, and U. Gerstmann, Phys. Stat. Sol. C **5**, 2358 (2008).

[28] S. Sanna, W. G. Schmidt, Th. Frauenheim, and U. Gerstmann, Phys. Rev. B **80**, 104120 (2009).

[29] R. Jones and B. Hourahine, in *Rare-earth Doped III-nitrides for Optoelectronic and Spintronic Applications*, edited by K. O'Donnell and V. Dierolf (Springer, Netherlands, 2010).

[30] C. G. Van de Walle and J. Neugebauer, J. Appl. Phys. **95**, 3851 (2004).

[31] I. C. Diallo and D. O. Demchenko, Phys. Rev. Applied **6**, 064002 (2016).

[32] A. Thiess, P. H. Dederichs, R. Zeller, S. Blügel, and W. R. L. Lambrecht, Phys. Rev. B **86**, 180401(R) (2012).

[33] R. Wakamatsu, D. Timmerman, D. Lee, A. Koizumi, and Y. Fujiwara, J. Appl. Phys. **116**, 043515 (2014).

[34] N. Woodward, A. Nishikawa, Y. Fujiwara, and V. Dierolf, MRS Proc. **1342**, mrss11-1342-v05-06 (2011).

[35] V. Kachkanov, K. P. O'Donnell, C. Rice, D. Wolverson, R. W. Martin, K. Lorenz, E. Alves, and M. Bockowski, MRS Proc. **1290**, mrsf10-1290-i03-06 (2011).

[36] M. Ishii, A. Koizumi, and Y. Fujiwara, Appl. Phys. Lett. **105**, 171903 (2014).

[37] M. Ishii, A. Koizumi, and Y. Fujiwara, J. Appl. Phys. **117**, 155307 (2015).

[38] M. Ishii, A. Koizumi, and Y. Fujiwara, Appl. Phys. Lett. **107**, 082106 (2015).

[39] W. Kohn and L. J. Sham, Phys. Rev. **140**, A1133 (1965).

[40] G. Kresse and J. Furthmuller, Comput. Mater. Sci. **6**, 15 (1996).

[41] H. J. Monkhorst and J. D. Pack, Phys. Rev. B **13**, 5188 (1976).

[42] Y. K. Zhou, S. W. Choi, S. Emura, S. Hasegawa, and H. Asahi, Appl. Phys. Lett. **92**, 062505 (2008).

[43] L. Liu, P.Y. Yu, Z. Ma, and S. S. Mao, Phys. Rev Lett. **100**, 127203 (2008).

[44] J. K. Mishra, S. Dhar, M. A. Khaderabad, and O. Brandt, MRS Proc. **1290**, mrsf10-1290-i03-01 (2011).

[45] A. Kaminski and S. Das Sarma, Phys. Rev. Lett. **88**, 247202 (2002).

[46] D. Tao, C. Liu, C. Yin, and J. Li, Mater. Lett. **114**, 22 (2014).